DALTON
FULL PAPER

Hydrothermal synthesis, structure and characterization of a novel layered vanadium oxide with metal coordination complexes: $[Ni(en)_2][V_6O_{14}]$

Bi-Zhou Lin *[a,b] and Shi-Xiong Liu [a]

[a] *Department of Chemistry, Fuzhou University, Fuzhou 350002, P. R. China*
[b] *Institute of Material Physical Chemistry, Huaqiao University, Quanzhou 362011, P. R. China. E-mail: bzlin@hqu.edu.cn*

Received 4th July 2001, Accepted 7th December 2001
First published as an Advance Article on the web 13th February 2002

The hydrothermal reaction of V_2O_5, $Ni(NO_3)_2{\cdot}6H_2O$, ethylenediamine and H_2O in the molar ratio of 1:1:3.5:519 at 180 °C yields black plates of $[Ni(en)_2][V_6O_{14}]$. This compound has been characterized structurally, magnetically, electrically, and spectroscopically. The crystal structure consists of novel mixed-valence vanadium oxide layers and interlayer metal coordination complexes. Each of the three VO_5 square pyramids share two edges to form a V_3O_{11} group. The V_3O_{11} groups are connected through sharing edges to produce a linear ribbon. Adjacent strips share corners to form a layer structure. The two oxygen atoms from the neighbouring vanadium oxide layers are coordinated to each nickel atom in a *trans*-fashion, and form a three-dimensional framework structure. An EHT (Extended Hückel Theory) calculation was performed to analyze the electronic structure, and the electrical resistivity measurements confirmed the expected semiconducting behavior of $[Ni(en)_2][V_6O_{14}]$.

Introduction

The intense contemporary interest in the self-assembly of inorganic molecular precursors or subunits [1] is a major driving force behind significant efforts directed toward the design and development of synthetic strategies [2] for systems with novel structural and topological properties. It has been demonstrated that the utilization of polar organic molecules for the structure direction of inorganic solids has been of great value in the assembly of microporous materials such as zeolites,[3] bio-mineralized compounds [4] and transition metal phosphates.[5] On the other hand, the development of new and open frameworks of transition metal oxides with wide variable oxidation states is particularly attractive for their catalytic, magnetic, electronic, intercalation or ion-exchange properties,[6] which can lead, for example, to the development of new cathode materials for Li-batteries.[7] Prompted by such considerations, organically directed transition metal oxides have been well synthesized in the past few years.[8–10] However, examples of vanadium oxides assembled with metal coordination complexes are still rare. They include one-dimensional metavanadate chain compounds $Cu(en)(VO_3)_2$, $Cu(2,2'\text{-bpy})(VO_3)_2$, $Cu(2,2'\text{-bpy})_2(VO_3)_2$,[11] $Cu(dien)(VO_3)_2$ [12] and $Ni(NH_3)_2(VO_3)_2$,[13] in which the Cu(II) or Ni(II) complexes are attached to the inorganic chains. Some new mixed-valance vanadium oxide layers have also been observed in $[Cu(en)_2][V_6O_{14}]$, $[Zn(en)_2][V_6O_{14}]$, $[Cu(en)_2][V_{10}O_{25}]$ [14] and $[Cd(enMe)_2][V_8O_{20}]$,[15] where the intercalated metal/organic fragments are incorporated directly into the covalent backbone of the solids as complex bridging ligands. Associated with the remarkable diversities in the coordination geometry of vanadium in various oxidation states, the second metal ions as well as the organic molecules can exert significant influence on the geometric topology of vanadium oxides. Hence, it is considerably appealing to exploit novel assembly systems of vanadium oxides with metal/ligand coordination groups through modifying the second metal ions, the organic ligands, the reducing reagents and the synthetic conditions. We report herein the hydrothermal synthesis, crystal structure, band structure and some important physical properties of a novel layered vanadium oxide $[Ni(en)_2][V_6O_{14}]$, where the Ni(II) coordination complexes are covalently bonded to the layers, generating a three-dimensional framework structure.

Experimental

Materials and methods

Regents were purchased commercially and used without further purification. The hydrothermal reactions were carried out in 17 mL Teflon-lined stainless steel autoclaves under autogenous pressure with a fill factor of approximately 40%. The reactants were stirred briefly before heating. Elemental analyses were performed on a Perkin-Elmer 2400 element analyzer and inductively coupled plasma analysis on a Perkin-Elmer Optima 3300DV ICP spectrometer. Infrared spectra were recorded at room temperature on a Perkin-Elmer FT-IR 2000 spectrophotometer as KBr pellets in the 4000–400 cm^{-1} region. Electrical resistivities were measured from 273 to 533 K by a conventional dc four-probe method. Electrical contracts were made using silver paste. Magnetic susceptibility data were obtained using a Quantum Design PPMS 6000 magnetometer in the temperature range from 4 to 275 K at an applied magnetic field of 5 kG whereby the diamagnetic contributions were estimated from Pascal's constants.

Synthesis

A mixture of V_2O_5 (0.136 g), $Ni(NO_3)_2{\cdot}6H_2O$ (0.218 g), ethylenediamine (0.15 mL) and H_2O (7.0 mL) in the molar ratio of 1:1:3.5:519 was heated at 180 °C for 52 h. The pH values of the medium were about 8.0 before and after the reaction. The product was black, plate-shaped crystals of $[Ni(en)_2][V_6O_{14}]$ as the major phase along with a green polycrystalline material (*ca.* 5% by visual observation) that has not been further characterized. The crystals were separated mechanically, washed with water and dried in air at ambient temperature. The yield of the title compound was *ca.* 80% based on vanadium. Anal. calc. for $C_4H_{16}N_4NiO_{14}V_6$: C, 6.78; H, 2.28; N, 7.91; Ni, 8.28; V, 43.14%. Found: C, 6.75; H, 2.31; N, 7.83; Ni, 8.24; V, 43.23%.

DOI: 10.1039/b105934n

Table 1 Summary of crystallographic data for $[Ni(en)_2][V_6O_{14}]$

Empirical formula	$C_4H_{16}N_4NiO_{14}V_6$
M	708.56
T/K	296(2)
Crystal system	Orthorhombic
Space group	*Cmca*
a/Å	16.597(3)
b/Å	6.6200(10)
c/Å	17.117(3)
V/Å^3	1880.7(6)
Z	4
D_c/Mg m^{-3}	2.502
μ/mm^{-1}	3.905
$R_1(F_o)$	0.0559
$wR_2(F_o^2)$	0.1309

Table 2 Selected bond lengths (Å) and angles (°) for $[Ni(en)_2][V_6O_{14}]$

Ni(1)–N(1)	2.032(10)	Ni(1)–O(1)	2.105(8)
V(1)–O(1)	1.603(8)	V(1)–O(3d)	1.841(10)
V(1)–O(3)	1.912(10)	V(1)–O(2b)	1.976(5)
V(1)–O(2)	1.976(5)	V(2)–O(4)	1.576(6)
V(2)–O(5)	1.803(2)	V(2)–O(2e)	1.867(6)
V(2)–O(2)	1.877(6)	V(2)–O(3)	2.471(2)
V(1) ··· V(2)	3.083(2)	N(1) ··· O(4g)	3.051(11)
N(1) ··· O(4c)	3.052(10)		
N(1a)–Ni(1)–N(1)	95.0(5)	N(1b)–Ni(1)–N(1)	85.0(5)
N(1c)–Ni(1)–N(1)	180.0	N(1a)–Ni(1)–O(1)	90.5(3)
N(1b)–Ni(1)–O(1)	89.5(3)	N(1c)–Ni(1)–O(1)	90.5(3)
N(1)–Ni(1)–O(1)	89.5(3)	O(1c)–Ni(1)–O(1)	180.0
O(1)–V(1)–O(3d)	113.3(4)	O(1)–V(1)–O(3)	112.4(4)
O(3d)–V(1)–O(3)	134.3(2)	O(1)–V(1)–O(2b)	104.44(18)
O(3d)–V(1)–O(2b)	83.39(18)	O(3)–V(1)–O(2b)	85.5(2)
O(1)–V(1)–O(2)	104.44(18)	O(3d)–V(1)–O(2)	83.39(19)
O(3)–V(1)–O(2)	85.5(2)	O(2b)–V(1)–O(2)	151.0(4)
O(4)–V(2)–O(5)	108.6(3)	O(4)–V(2)–O(2e)	111.2(3)
O(5)–V(2)–O(2e)	99.1(4)	O(4)–V(2)–O(2)	110.6(3)
O(5)–V(2)–O(2)	98.5(4)	O(2e)–V(2)–O(2)	126.0(2)
O(4)–V(2)–O(3)	95.4(3)	O(5)–V(2)–O(3)	155.9(3)
O(2e)–V(2)–O(3)	70.1(3)	O(2)–V(2)–O(3)	73.3(3)
V(1)–O(1)–Ni(1)	175.2(5)	V(2d)–O(2)–V(2)	142.9(3)
V(2d)–O(2)–V(1)	110.5(3)	V(2)–O(2)–V(1)	106.3(3)
V(1e)–O(3)–V(1)	145.3(6)	V(1e)–O(3)–V(2)	93.0(2)
V(1)–O(3)–V(2)	88.4(2)	V(2)–O(5)–V(2f)	174.4(7)
C(1)–N(1)–Ni(1)	97.1(7)	N(1)–H(1)–O(4g)	134.0(2)
N(1)–H(2)–O(4c)	155.9(5)		

Symmetry codes: (a) $x, -y, -z + 1$; (b) $-x + 1, y, z$; (c) $-x + 1, -y, -z + 1$; (d) $x, y - 1/2, -z + 1/2$; (e) $x, y + 1/2, -z + 1/2$; (f) $-x + 1/2, y, -z + 1/2$; (g) $-x + 1, y - 1, z$.

X-Ray crystallography

The crystal structure of $[Ni(en)_2][V_6O_{14}]$ was determined by single crystal X-ray diffraction methods. The data on a crystal with dimensions 0.62 × 0.25 × 0.10 mm were collected on a Rigaku AFC5R four-circle diffractometer with graphite monochromated Mo Kα radiation (λ = 0.71069 Å), the scan mode being ω–2θ at a scan speed of 6 ° min^{-1} in ω. Cell dimensions were refined using 25 reflections in the range $20 < 2\theta < 30°$. Three standard reflections were monitored every 100 reflections to give no significant intensity deviations. A total of 1060 reflections ($2\theta_{max}$ = 52°) were collected, of which 956 unique reflections (R_{int} = 0.0462) were used for structural elucidation. The diffraction data were corrected for Lorentz-polarization effects, and empirical absorption corrections[16] based on φ-scans were applied.

The structure was solved in the orthorhombic space group *Cmca* by direct methods using the SHELXS-86 software package.[17] All non-hydrogen atoms were refined anisotropically. The hydrogen atoms were located in the difference Fourier map and were included in the refinement with fixed positional and thermal parameters. The refinement of the structure was run on F^2 by full-matrix, least-square techniques using the SHELXL-97 crystallographic software package.[18] At convergence, R_1 = 0.0559 and the goodness of fit on F^2 was 1.024. A summary of the crystallographic data is given in Table 1. Selected bond lengths and angles are listed in Table 2.

CCDC reference number 178356.

See http://www.rsc.org/suppdata/dt/b1/b105934n/ for crystallographic data in CIF or other electronic format.

Results and discussion

Synthesis and IR spectrum

Hydrothermal reactions, typically performed in the temperature range 120–300 °C under autogenous pressure, exploit the self-assembly of the products from soluble precursors.[2,19] The reduced viscosity of water under hydrothermal conditions enhances the solvent extraction of solids and the rate of crystallization from solution. A variety of starting materials may be introduced since most species are soluble under these conditions employed. While the mechanism by which the assembly is organized remains elusive, in combination with the structure-directing templates, the hydrothermal synthesis methodology has been demonstrated to be a useful approach to employing organic components to modify the crystallization of metal oxides.[20] The synthetic results, however, are sensitive to many parameters such as the starting materials, templates, pH, temperature and pressure. It was observed that the pH value of the reaction mixture plays a critical role on the V_2O_5–$Ni(NO_3)_2$–en–H_2O system for reactions at 175 °C for 3 days. The pH values were controlled at *ca.* 8.0 in order to isolate $[Ni(en)_2][V_6O_{14}]$ as the major phase. In contrast, $[H_2en][V_4O_{10}]$, which was reported earlier,[10] was found from reaction at a pH of 7.0–7.5, and $Ni(en)_3(VO_3)_2$ was obtained as the major phase at the pH of 8.2–9.0.[21] This suggests that there be a strong competition between formation of the different solid phases in this synthetic system. It is thus difficult to yield the mono-phase of $[Ni(en)_2][V_6O_{14}]$ without the by-product. Nevertheless, the optimum conditions for preparing $[Ni(en)_2][V_6O_{14}]$ are a mixture of V_2O_5, $Ni(NO_3)_2{\cdot}6H_2O$, en and H_2O in the molar ratio of 1:1:3.5:519 and reaction at 180 °C for 52 h. Although an extensive study was carried out, attempts to characterize the by-product observed were unsuccessful.

In the IR spectrum of the title compound (not shown), strong bands at 1009 and 967 cm^{-1} are assigned to the terminal V=O stretching in VO_5 square pyramids, the former band corresponding to V(2)–O(4) and the latter to V(1)–O(1). Apart from a longer V=O distance as listed in Table 2, the reduced absorption frequency of V(1)–O(1) may be derived from the covalent connections between O(1) and Ni atoms in the crystal structure of the title compound (as shown below). Features at 872 and 759 cm^{-1} are related to the symmetric and antisymmetric stretching of V–O–V. These stretching bands are in accord with those observed in polyoxovanadates, which are constructed from VO_5 square pyramids.[22] Bands ranging from 1275 to 1578 cm^{-1} are attributed to C–C stretching, and those at 1092 and 1150 cm^{-1} to C–N stretching, whereas the band at 2895 cm^{-1} is assigned to C–H stretching, and that at 3257 cm^{-1} to N–H stretching.

Crystal structure

The structure of $[Ni(en)_2][V_6O_{14}]$ consists of novel vanadium oxide layers with $Ni(en)_2^{2+}$ complexes located in the interlayer positions. The coordination environments around the vanadium and nickel atoms in the asymmetric unit are depicted in Fig. 1. Two crystallographically independent vanadium sites V(1) and V(2) both exhibit a distorted square pyramidal geometry. Atoms O(2), O(2b), O(3) and O(3d) are coordinated to V(1), forming a basal plane with V–O bond lengths ranging from 1.841(10) to 1.976(6) Å. The apical position is located by O(1) with the shortest bond distance of 1.603(8) Å. Atoms

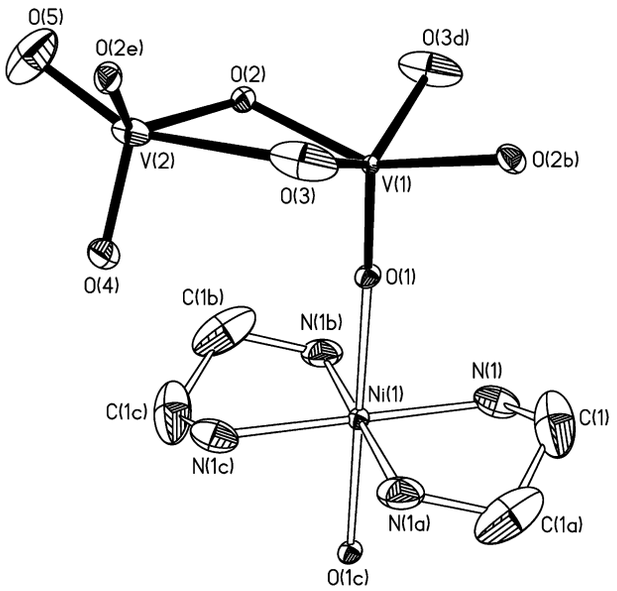

Fig. 1 Asymmetric unit in $[Ni(en)_2][V_6O_{14}]$, showing the metal-atom coordination environments with 50% probability displacement ellipsoids.

V(1), O(1), O(3) and O(3d) are on a mirror plane. In the square pyramid around V(2), the four basal V–O bond distances are between 1.803(2) and 2.471(2) Å, while the terminal O(4) atom is in the axial position with a V=O bond length of 1.576(6) Å. The polyhedron distortions are 0.58 for V(1) and 0.55 for V(2), according to Mutterties and Guggenberger's calculating method.[23] The coordination octahedron around each nickel atom has C_{2v} symmetry. The four equatorial nitrogen atoms come from two ethylenediamine ligands each with a Ni–N bond distance of 2.032(10) Å, and the two axial oxygen atoms from the apical oxygen atoms of two adjacent vanadium oxide layers each having a Ni–O bond length of 2.105(8) Å.

The inorganic layers formulated by $[V_6O_{14}]^{2-}$ are composed solely of VO_5 square pyramids. Fig. 2 shows a view perpendicular to one of the vanadium oxide layers. The layer structure can be described as being connected by V_3O_{11} building groups. Within a V_3O_{11} group, the middle VO_5 square pyramid shares each of its two adjacent basal edges with another pyramid, exhibiting a 'V' shape with their three apical oxygen atoms pointing up the same sides of the plane of the vanadium oxide layers. The V_3O_{11} groups are connected through sharing edges to produce a linear ribbon along the *b* axis. In the ribbon, the apical oxygen atoms of the neighboring V_3O_{11} groups are oriented towards opposite sides of the plane of the layers. If these two relative orientations are respectively labeled 'up' and 'down', the arrangement of the V_3O_{11} groups in the ribbon is in the row of up–down–up–down$\cdots$ Adjacent strips further share their peripheral corners along the *a* axis into a layer structure. Along the *a* axis, the arrangement of the V_3O_{11} groups is also in the rows of up–down–up–down$\cdots$ This vanadium oxide layer structure in $[Ni(en)_2][V_6O_{14}]$ is distinctly different from those with similar compositions. The $[V_3O_7]^-$ or $[V_6O_{14}]^{2-}$ layers found in compounds $[NN(C_2H_4)_3NH][V_6O_{14}]\cdot H_2O$,[24] $[NMe_4][V_3O_7]$,[25] $[N(CH_3)_4]_2[Co(H_2O)_4V_{12}O_{28}]$,[26] $[Cu(en)_2][V_6O_{14}]$ and $[Zn(en)_2][V_6O_{14}]$[14] are built up from VO_4 tetrahedra and VO_5 square pyramids *via* sharing edges and corners. The $[V_3O_7]^-$ layers in MV_3O_7 (M = Ca, Sr and Cd) are also made up solely of VO_5 square pyramids.[27,28] However, the polyhedral connections in the title compound are dissimilar. Whereas the pyramids in MV_3O_7 (M = Ca, Sr and Cd) are linked through sharing edges, the ones in our case are linked through sharing edges and corners. It should be pointed out that atom O(3) in $[Ni(en)_2][V_6O_{14}]$ is shared by four vanadium atoms, as shown in Fig. 2. This coordination number of oxygen atoms is very rare in vanadates. To our knowledge, such linkages have only been observed in the structures of $Li_xV_3O_8$ ($x = 1.5$),[29] $H_2V_3O_8$[30] and β-$AgVO_3$,[31] in which some of the bridging oxygen atoms are shared by four VO_6 octahedra. $[Ni(en)_2][V_6O_{14}]$ provides a new example with some of the bridging oxygen atoms shared by four VO_5 square pyramids.

Fig. 3 displays the framework structure of $[Ni(en)_2][V_6O_{14}]$.

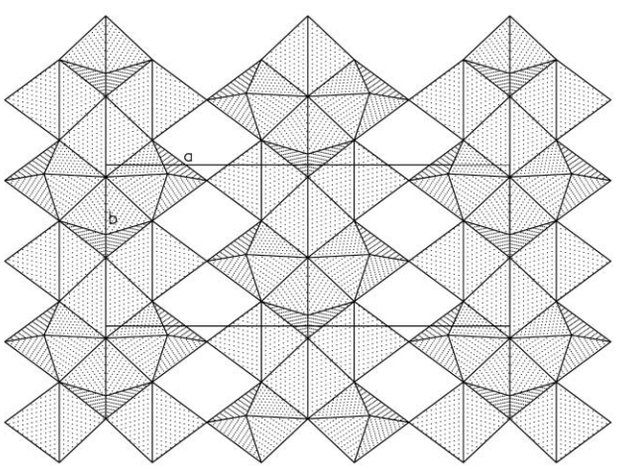

Fig. 2 Polyhedral representation of a $[V_6O_{14}]^{2-}$ layer in $[Ni(en)_2][V_6O_{14}]$ along the *c* axis, showing the connections of VO_5 pyramids.

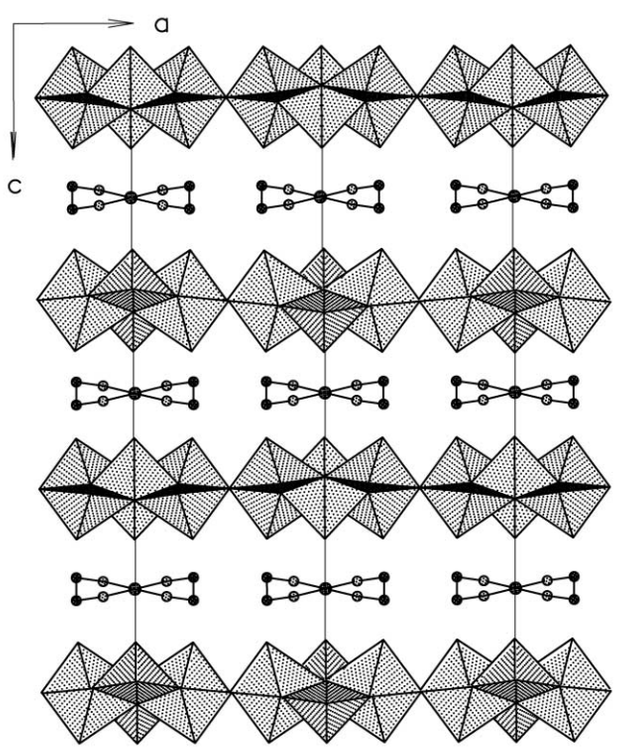

Fig. 3 Projection of $[Ni(en)_2][V_6O_{14}]$ along the *b* axis, showing the vanadium oxide layers connected by Ni complexes into a 3-D framework with 1-D channels.

The vanadium oxide layers are covalently connected by Ni atoms into a three-dimensional open framework. The linkage between oxygen atoms and nickel atoms is relatively strong with a distance of 2.105(8)Å. This arrangement gives one-dimensional channels along the *b* axis with 10-membered rings composed of O–O edges of eight VO_5 square pyramids and two NiO_2N_4 octahedra or 20-membered rings counting metal and oxygen atoms individually. The distance between the neighboring vanadium oxide layers is 8.559(3) Å. The coordination fashion of oxygen atoms from the vanadium oxide layers to the metal atoms of the coordination complexes in $[Ni(en)_2][V_6O_{14}]$

is similar to that in other layered vanadium oxides incorporating six-coordinated interlamellar complex cations, namely $[N(CH_3)_4]_2[Co(H_2O)_4V_{12}O_{28}]$,[26] $[Cu(en)_2][V_6O_{14}]$, $[Zn(en)_2][V_6O_{14}]$ and $[Cu(en)_2][V_{10}O_{25}]$,[14] but it is different from that in $[Ni(2,2'\text{-bpy})_2][V_6O_{17}]$[32] and $[Zn(2,2'\text{-bpy})_2][V_6O_{17}]$.[14] In the structures of the latter compounds, the two oxygen atoms come from a single vanadium oxide layer and are coordinated to each second metal atom in a *cis*-fashion, maintaining the two-dimensional network structures. In contrast, in $[Ni(en)_2][V_6O_{14}]$, the two oxygen atoms come from the two adjacent vanadium oxide layers and are bonded to each nickel atom in a *trans*-fashion, forming a three-dimensional framework structure. There is extensive hydrogen bonding between the N–H groups from the complexes and the oxygen atoms from the inorganic layers in $[Ni(en)_2][V_6O_{14}]$ with N ··· O interatomic distances of 3.051(11) and 3.052(10) Å, as listed in Table 2.

Magnetic and electrical properties

The magnetic behavior of $[Ni(en)_2][V_6O_{14}]$ is illustrated in Fig. 4.

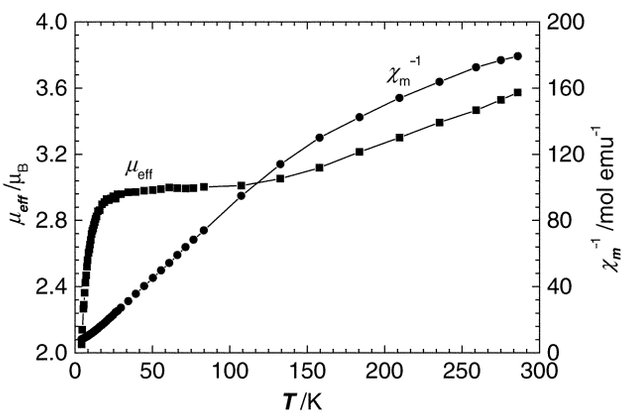

Fig. 4 Thermal variations of the molar effective magnetic moment (μ_{eff}) and inverse susceptibility data (χ_m^{-1}) of $[Ni(en)_2][V_6O_{14}]$.

The molar effective magnetic moment (μ_{eff}) decreases nearly linearly with decreasing temperature from 3.57 μ_B at 285 K to 3.02 μ_B at 130 K. While the μ_{eff} value remains at about 3.02 μ_B between 130 and 25 K, it decreases rapidly from 25 K and reaches a value of 2.05 μ_B at near 4 K. According to the valence sum calculations[33] and the charge balance, a layer composition in $[Ni(en)_2][V_6O_{14}]$ should be $[V^{5+}{}_2V^{4+}{}_4O_{14}]^{2-}$. But even at 285 K, the μ_{eff} value is still below that expected (4.47 μ_B) for the six unpaired spins from one Ni(II) and four V(IV) ions. The magnetic moment of 3.02 μ_B between 130 and 25K is only slightly greater than that expected (2.86 μ_B) for the Ni(II) ion with $S = 1$. In general, such magnetic behavior may suggest that either the vanadium oxide layers have already undergone a strong antiferromagnetic transition above room temperature or that the spins are paired within states that are delocalized within the layers. As described below, the EHT (Extended Hückel Theory) calculations reveal that this magnetic observation may be derived from both cases. It is interesting that the shape of the magnetic moment below 25 K in Fig. 4 is qualitatively similar to that expected for an isolated Ni(II).[21] It thus seems that its temperature dependencies come basically from a zero-field splitting model, where the $M_s = 0$ state lies below the $M_s = \pm 1$ states in the nickel octahedral field. Since the electron states within the vanadium oxide layers are delocalized, it is difficult to quantifiably analyze the magnetic data.

As shown in Fig. 5, $[Ni(en)_2][V_6O_{14}]$ exhibits an anisotropically electron-conductive characteristic. At certain temperatures, the electrical resistivity along the *a* axis is about four times greater than that along the *b* axis. The resistivities along the two directions above lie in the order of 10^{-2} Ω cm and between 10^{-3} and 10^{-2} Ω cm in the measured temperature range from 275 to 525 K, respectively. According to the definition by Kittel,[34] the electrical resistivity of semiconductors is 10^{-5} to 10^{7} Ω cm; $[Ni(en)_2][V_6O_{14}]$ resistivities are extrinsic semiconductor values.

Table 3 Atomic parameters employed in the EHT calculation

Atom	Orbital	H_{ii}/eV	ζ_{11} (c_1)	ζ_{12} (c_2)
V	4s	−8.81	1.300	
	4p	−5.54	1.300	
	3d	−11.00	4.750 (0.4755)	1.700 (0.7052)
O	2s	−32.30	2.275	
	2p	−14.80	2.275	

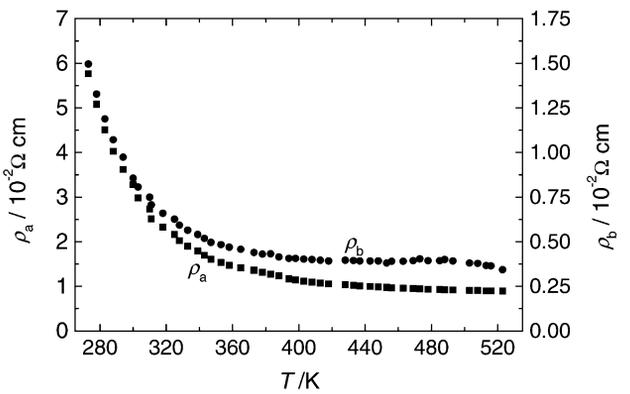

Fig. 5 Thermal variations of the electrical resistivity of $[Ni(en)_2][V_6O_{14}]$.

The tight-binding band structure was calculated on the vanadium oxide layers in $[Ni(en)_2][V_6O_{14}]$ by the EHT crystal orbital method (Table 3).[35] The band structure near the Fermi level ($E_f = -10.36$ eV) is presented in Fig. 6. The Fermi level

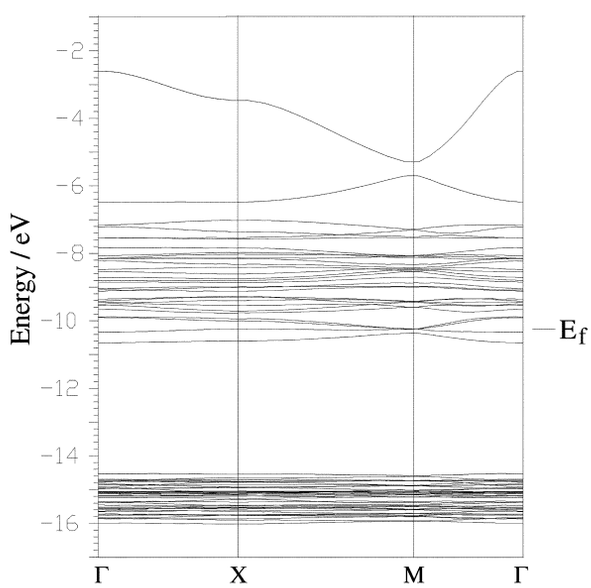

Fig. 6 The band structure of $[V_6O_{14}]^{2-}$ in $[Ni(en)_2][V_6O_{14}]$.

crosses two conduction bands along the direction from X(0.5, 0, 0) to M(0.5, 0,5, 0), but it does not cross any conduction band along that from Γ(0, 0, 0) to X(0.5, 0, 0). Compared with the valence bands below −14eV, the crossed conduction bands are delocalized with gaps about 0.4eV wide. This indicates that the title compound is expected to have good electron-conductibility and that it has distinctly different electron-conductivities along the *a* and *b* axes, which is in good agreement with the resistivity observations.

The diagrams of the total and projected density of states (DOS) are displayed in Fig. 7. The two upper valence bands and the conduction bands are essentially composed of V 3d and

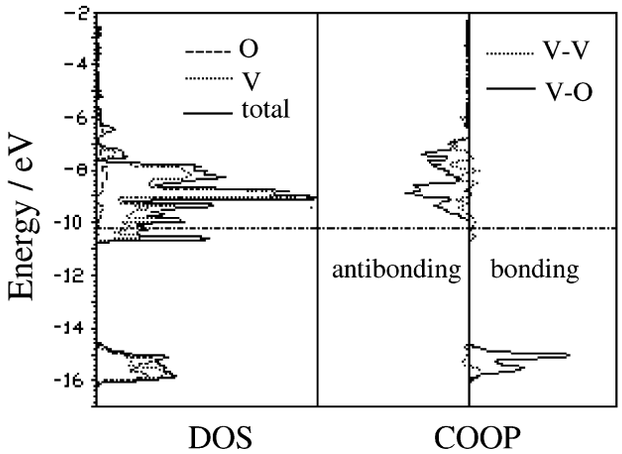

Fig. 7 Selected DOS and COOP curves for $[Ni(en)_2][V_6O_{14}]$.

O 2p orbitals with more contributions from vanadium atoms, whereas the valence bands in the energy interval from −16 to −14 eV are primarily constructed from V–O covalent bonding. The crystal orbital overlap population (COOP) curves in Fig. 7 show that V–O bonding is optimized, i.e. all of the bonding region is occupied and the antibonding one is empty. The COOP plot indicates that both V–V bonding and antibonding 3d states in the interval from −16 to −14 eV are occupied, and that the antibonding states are slightly weaker than the corresponding bonding ones owing to the second-order mixing of the V 4s and 4p orbitals into 3d orbitals. On the other hand, the V–V bonding 3d states at the top of the valence bands are also occupied. As a consequence, the integrated COOP gives the small positive value of 0.035 for the V ··· V contact of 3.083(2)Å. Although the metal–metal interactions are weak with this small positive number, the d–d orbital overlap is significant enough to make a strong antiferromagnetic coupling between the paramagnetic centers. Furthermore, the metal–metal interactions extend along the *b* axis, making the two upper valence bands and most conduction bands delocalized (Fig. 6). The delocalized states thus result in the spins being paired within the vanadium oxide layers and indicate that the title compound has a semiconducting characteristic in electron conductibility. The EHT calculations are in accord with the magnetic and electrical measurements.

In summary, this paper presents a new example of hydrothermally assembling vanadium oxides through the templating effect of transition metal complexes for the isolation of composite organic/inorganic solids. The title compound is built up of novel vanadium oxide layers intercalated by $Ni(en)_2^{2+}$ complexes, where the Ni(II) groups are covalently incorporated to the layers, giving a three-dimensional framework structure. It demonstrates the availability of the hydrothermal methods for the efficient preparation of new materials with novel structural and topological features.

Acknowledgements

The authors thank the Natural Science Foundation of Fujian Province of China under Grant No. D0010010 for financial support.

References

1 A. Müll and H. Reuter, *Angew. Chem., Int. Ed. Engl.*, 1995, **34**, 2328.
2 A. Atein, S. W. Keller and T. E. Mallouk, *Science*, 1990, **67**, 829; J. Gopalakrishnan, *Chem. Mater.*, 1995, **7**, 1265.
3 J. V. Smith, *Chem. Rev.*, 1988, **88**, 149.
4 S. Mann, *Nature*, 1993, **365**, 499.
5 R. C. Haushalter and L. A. Mundi, *Chem. Mater.*, 1992, **4**, 31; J. Zubieta, *Comments Inorg. Chem.*, 1994, **16**, 153; G. D. Stucky, *Nature*, 1997, **388**, 691; Z. Shi, S. Feng, S. Gao, L. Zhang, G. Yang and J. Hua, *Angew. Chem., Int. Ed.*, 2000, **39**, 2325.
6 S. L. Suib, *Chem. Rev.*, 1993, **93**, 803; D. W. Murphy and P. A. Chirstian, *Science*, 1979, **205**, 651; A. Stain, S. W. Keller and T. E. Wallouk, *Science*, 1993, **259**, 1558; E. Canadell, J. Provost, A. Guesdon, M. M. Borel and A. Leclaire, *Chem. Mater.*, 1997, **9**, 68; T. Chirayil, P. Zavalij and M. Whittingham, *Solid State Ionics*, 1996, **84**, 163.
7 W. Li, J. R. Dahn and D. S. Wainwright, *Science*, 1994, **264**, 1115.
8 I. W. C. E. Arends, R. A. Sheldon and M. Wallau Schuchardt, *Angew. Chem., Int. Ed. Engl.*, 1997, **36**, 1144; M. Hartman and L. Kevan, *Chem. Rev.*, 1999, **99**, 635; P. J. Hagrman and J. Zubieta, *Inorg. Chem.*, 2000, **23**, 5218.
9 T. Chirayil, P. Y. Zavalij and M. S. Whittingham, *J. Mater. Chem.*, 1997, **7**, 2193; Y. Zhang, C. J. O'Connor, A. Clearfield and R. C. Haushalter, *Chem. Mater.*, 1996, **8**, 595.
10 D. Riou and G. Férey, *Inorg. Chem.*, 1995, **34**, 6520; Y. Zhang, R. C. Haushalter and A. Clearfield, *Inorg. Chem.*, 1996, **35**, 4950.
11 J. R. D. DeBord, Y. Zhgang, R. C. Haushalter, J. Zubieta and C. J. O'Connor, *J. Solid State Chem.*, 1996, **122**, 251.
12 L. M. Zheng, J. Z. Zhao, K. H. Lii, L. Y. Zhang, Y. Liu and X. Q. Xin, *J. Chem. Soc., Dalton Trans.*, 1999, 939.
13 B. Z. Lin and S. X. Liu, *Polyhedron*, 2000, **19**, 2527.
14 Y. Zhang, J. R. D. DeBord, C. J. O'Connor, R. C. Haushalter, A. Clearfield and J. Zubieta, *Angew. Chem., Int. Ed. Engl.*, 1996, **35**, 989.
15 L. Zhang, Z. Shi, G. Yang, X. Chen and S. Feng, *J. Chem. Soc., Dalton Trans.*, 2000, 275.
16 A. C. T. North, E. C. Phillips and F. S. Mathews, *Acta Crystallogr., Sect. A*, 1968, **24**, 351.
17 G. M. Sheldrick, *Acta Crystallogr., Sect. A*, 1990, **46**, 467.
18 G. M. Sheldrick, SHELXL-97, Program for Refinement of Crystal Structures, University of Göttingen, Germany, 1997.
19 A. Rabenau, *Angew. Chem., Int. Ed. Engl.*, 1985, **24**, 1026.
20 P. J. Hagrman, D. Hagrman and J. Zubieta, *Angew. Chem., Int. Ed.*, 1999, **38**, 2638.
21 S. X. Liu, B. Z. Lin and S. Lin, *Inorg. Chim. Acta*, 2000, **304**, 33.
22 A. Müller, R. Rohlfing, E. Krichemeyer and H. Bögge, *Angew. Chem., Int. Ed. Engl.*, 1987, **26**, 1045; T. Yamase and K. Ohtaka, *J. Chem. Soc., Dalton Trans.*, 1994, 2599; A. Müller, R. Sessoli, E. Krickemeyer, H Bögge, J Meyer, D. Gatteschi, L. Pardi, J. Westphal, K. Hovemeier, R. Rohlfing, J. Döring, F. Hellweg, C. Beugholt and M. Schmidtmann, *Inorg. Chem.*, 1997, **36**, 5239.
23 E. L. Mutterties and L. J. Guggenberger, *J. Am. Chem. Soc.*, 1974, **96**, 1748 and references therein.
24 L. F. Nazar, B. E. Koene and J. F. Britten, *Chem. Mater.*, 1996, **8**, 327; Y. Zhang, R. C. Haushalter and A. Clearfield, *Chem. Commun.*, 1996, 1055.
25 T. G. Chirayil, E. A. Boglan, M. M. Peter, P. Y. Zavalij and M. S. Whittingham, *Chem. Commun.*, 1997, 33.
26 X. Wang, L. Liu, A. J. Jacobson and K. Ross, *J. Mater. Chem.*, 1999, **9**, 859.
27 J. C. Bouloux and J. Galy, *Acta Crystallogr., Sect. B*, 1973, **29**, 269.
28 G. Liu and J. E. Greedan, *J. Solid State Chem.*, 1993, **103**, 139.
29 A. D. Wadsley, *Acta Crystallogr.*, 1957, **10**, 261.
30 Y. Oka, T. Yao and N. Yamamoto, *J. Solid State Chem.*, 1990, **89**, 372.
31 P. Rozier, J.-M. Savariault and J. Galy, *J. Solid State Chem.*, 1996, **122**, 303.
32 B. Z. Lin and S. X. Liu, *Acta Crystallogr., Sect. C*, 2001, **57**, 243.
33 I. D. Brown and D. Altermatt, *Acta Crystallogr., Sect. B*, 1985, **41**, 244.
34 C. Kittel, *Solid State Physics*, Wiley, New York, 5th edn., 1976.
35 R. Hoffmann, *J. Chem. Phys.*, 1963, **39**, 1397; J. K. Burdett and S. Lee, *J. Am. Chem. Soc.*, 1983, **105**, 1079; J. K. Burdett and T. J. Mclarnan, *Inorg. Chem.*, 1982, **21**, 1119.